Scripta Materialia 143 (2018) 117–121

Contents lists available at ScienceDirect

Scripta Materialia

journal homepage: www.elsevier.com/locate/scriptamat

Regular article

Carbide precipitation characteristics in additive manufacturing of Co-Cr-Mo alloy via selective election beam melting

X.P. Tan [a,*], P. Wang [b], Y. Kok [a], W.Q. Toh [a], Z. Sun [a], S.M.L. Nai [b], M. Descoins [c], D. Mangelinck [c], E. Liu [a], S.B. Tor [a]

[a] Singapore Centre for 3D Printing, School of Mechanical and Aerospace Engineering, Nanyang Technological University, 50 Nanyang Avenue, 639798, Singapore
[b] Singapore Institute of Manufacturing Technology, 73 Nanyang Drive, 637662, Singapore
[c] IM2NP, UMR 7334 CNRS, Université Aix-Marseille, 13397 Marseille Cedex 20, France

ARTICLE INFO

Article history:
Received 19 August 2017
Received in revised form 9 September 2017
Accepted 14 September 2017
Available online xxxx

Keywords:
3D printing
Electron beam methods
Atom probe tomography
Carbides
Precipitation

ABSTRACT

Carbide precipitation plays a key role in determining mechanical properties of Co-Cr-Mo alloy. Precipitation characteristics of carbides in selective electron beam melting (SEBM)-fabricated Co-Cr-Mo parts have been investigated by atom probe tomography and transmission electron microscopy. We observe co-existence of two types of carbides, i.e. $M_{23}C_6$ and M_6C, which are formed into continuous carbide thin films along columnar grain boundaries. The carbide thin film is found to precipitate coherently with one γ—Co grain while incoherently with another adjacent one. Moreover, columnar carbide chains or clusters consisting of nanometer-sized, cuboidal particles are precipitated coherently with surrounding γ—Co phase within interdendritic regions.

Co-Cr-Mo alloy is a class of important high-performance structural engineering materials as it is one of a very few metallic materials that can be used for biomedical, corrosion and high-temperature applications. It offers a combination of many advantageous properties such as high strength and hardness, excellent wear, corrosion and heat resistance, and good biocompatibility [1,2]. Thereinto, the remarkable mechanical properties were gained mainly owing to a large quantity of carbide precipitation in microstructure, while usually leading to poor formability and machinability in turn [3]. Thanks to the rapid technological advance in metal additive manufacturing (AM) (also known as metal three-dimensional (3D) printing) technologies in recent years, high added value but hard-to-machine materials like Ti-6Al-4 V and Co-Cr-Mo can be manufactured into near-net-shape complex parts with relative ease [4–10].

Selective electron beam melting (SEBM) is a disruptive powder-bed fusion AM technology for metals and alloys, which utilizes a high-energy density electron beam to selectively melt over metallic powder bed layer by layer, creating near-net-shape 3D objects in an automated, digital manner [11,12]. The microstructure of SEBM-built Co-Cr-Mo parts was comprised of columnar face-centred cubic (fcc) γ—Co grains with a large amount of $M_{23}C_6$-type carbides aligned along build direction within grains and at grain boundaries [13–16]. Gaytan et al. [13,14] sketched a 3D architecture for the carbides precipitated within interdendritic regions, but the precipitation of grain boundary carbides was paid insufficient attention in their study. The columnar γ—Co grains were preferentially oriented with ⟨001⟩ direction under as-built conditions for short builds. However, Sun et al. [15,16] reported that these anisotropic columnar γ—Co grains would transform into more stable, equiaxed hexagonal closed-packed (hcp) ε—Co grains with an Shoji-Nishiyama orientation relationship after aging treatments or long-term SEBM thermal processes. There are two intrinsic strengthening mechanisms for the Co-Cr-Mo alloy itself: solid solution strengthening by Cr and Mo additions and secondary phase strengthening resulted from various types of carbides such as M_6C, $M_{23}C_6$ and M_7C_3, and the latter is the dominant strengthening mechanism [2]. It is noted that many different types of carbides may form in Co-Cr-Mo alloys depending on carbon contents as well as heat treatments [17]. It was reported that as-SEBM-built Co-Cr-Mo samples were brittle and exhibited obvious anisotropic properties, but they showed better tensile properties after post heat treatments as compared to its wrought or as-cast forms [13,18]. Furthermore, our preliminary investigation also demonstrated that there existed strong anisotropic behavior for SEBM-built Co-Cr-Mo parts on both tensile and compressive properties, i.e. it was significantly weaker when testing direction was normal to the columnar grain boundaries [19]. It can be hypothesized that the anisotropy in mechanical properties must be attributed to the precipitation of carbides. Nevertheless, there are still very limited studies conducted on detailed precipitation behavior of carbides in SEBM processing of Co-Cr-Mo alloy, particularly for the grain boundary carbides. This work was initiated into investigation of carbide precipitation at atomic scale and aims to figure out their precipitation characteristics for Co-Cr-Mo alloy

* Corresponding author.
E-mail addresses: xptan@ntu.edu.sg, xptan1985@gmail.com (X.P. Tan).

https://doi.org/10.1016/j.scriptamat.2017.09.022

during SEBM process. It will help to elucidate the origin of anisotropy in mechanical properties and provide useful guidance to achieve better mechanical performance for SEBM-built Co-Cr-Mo parts.

Co-Cr-Mo block parts with a build length of 100 mm, a build thickness of 10 mm and a build height of 30 mm were fabricated on a start plate of 210 × 210 × 10 mm^3 via an A2XX EBM system (Arcam EBM, Möndal, Sweden) using the ASTM F75 CoCr powder supplied by the same company. A schematic of the A2XX EBM system is shown in Fig. 1a. Its build envelop is Φ420 × 380 mm^3. A standard build theme provided by Arcam EBM was adopted. SEBM build temperature was ~ 800–850 °C. The chemical compositions of Arcam ASTM F75 pre-alloyed Co-Cr-Mo powder are as follows: 28.50Cr-6.00Mo-0.25Ni-0.20Fe-0.22C-0.70Si-0.50Mn-0.15 N–Bal. Co (in wt%). The powder size ranges from 45 to 106 μm as shown in Fig. 1b. The detailed SEBM process can be found elsewhere [20].

Both image analysis and Archimedes methods were adopted to measure the relative density of SEBM-built parts. Optical microscopy (OM; ZEISS Axioskop 2 MAT), X-ray diffraction (XRD; PANalytical Empyrean; Cu Kα; step size of 0.013°), scanning electron microscopy (SEM; JEOL JMS-6700F; 20 kV) and transmission electron microscopy (TEM; JEOL-2010; 200 kV) were used to examine the microstructure of as-built Co-Cr-Mo parts that were sliced into cubes of 10 × 10 × 10 mm^3 and then were hot mounted. Metallographic samples were prepared by following the Struer's standard grinding and polishing procedures. Electro-etching was performed at room temperature using a 5% HCl solution under 2 V for ~10 s after polishing.

In order to examine the carbide precipitation behavior occurring close to as-built conditions, specimens for microstructural observation were taken at the middle section of ~5 mm away from the top build surface of the SEBM-built Co-Cr-Mo block part. Thin longitudinal specimen sections were ground to ~100 μm and then manually ground to ~50 μm with 1000# sand papers. Standard Φ3 mm TEM discs were punched out from the thin foils. The disc was then dimpled on both sides and then ion milled at 4–8°. Ion milling voltage was varied between 3.5 and 4.5 V. The compositions of grains and carbides were measured by energy-dispersive X-ray spectroscopy (EDS) equipped in the TEM. In addition, we employed atom probe tomography (APT) to identify the carbides from the view of chemical at atomic scale. APT specimens were prepared by focused ion beam (FIB) on a FEI Helios dual-beam via the lift-out technique and the micro-tips were prepared using the annular milling method to obtain an end radius of ~50 nm. APT specimens were analyzed at 40 K and a gauge pressure < 2e-11 Torr. Pulses of green laser light (532 nm wavelength) were applied at a 200 kHz repetition rate with an energy of 0.9 nJ pulse^{-1}, yielding an evaporation rate of 1.2%. We analyzed APT data using IVAS® 3.6.6 software and obtained compositional information employing the one-dimensional (1D) concentration profiles.

Fig. 1c shows that some spherical pores with an average size of ~10–20 μm were present randomly in the as-built Co-Cr-Mo samples. There is no obvious difference on porosity among XY, XZ or YZ planes. These pores could be resulted from the small bubbles that originally existed inside the Co-Cr-Mo powders through gas atomisation [5]. The image analysis method records a relatively smaller porosity of ~0.5% compared to the Archimedes method of ~0.8%. The real porosity value should drop within this range. Fig. 1d shows the cross-section (XY plane) microstructure of as-built Co-Cr-Mo sample. Grains at a scale of tens of micrometres in diameter are enclosed by "bold lines" which are carbides. Moreover, the "dark dots" dispersed regularly in a square form are carbide particles within the interdendritic regions of grains.

Due to the high thermal gradients and the rapid solidification rates involved in metal AM processes, columnar or cellular microstructure would appear in most of the metals and alloys [4]. For SEBM processing of Co-Cr-Mo alloy, fine columnar γ—Co grains consisting of cellular dendrites were formed due to the dendritic micro-segregation of Cr and Mo. Moreover, carbides were precipitated because of the segregation of carbon into interdendritic regions and grain boundaries. Fig. 2a shows the columnar grains along the build direction from XZ plane. Each columnar grain consists of cellular dendritic structures with constrained secondary arms. Carbides are found to be formed both at columnar grain boundaries and interdendritic regions. In terms of the microstructural observation at different planes, we found that the carbides had formed continuous carbide thin films with a thickness of ~100–200 nm at grain boundaries, separating the adjacent columnar grains. While the carbides formed at interdendritic regions tend to become long chains or clusters in morphology along the primary dendrites. It is worth noting that these carbides could hardly be detected by conventional X-ray analysis using bulk samples, indicating a low quantity of below ~5% in volume fraction. Fig. 2b shows an representative APT tip specimen that was cut from the grain boundary carbide thin film. Accordingly, we obtained the APT reconstructed volume as shown in Fig. 2c. For simplicity, only the four main elements were indicated. Here, 50 at.% Co and 40 at.% Cr isoconcentration surfaces (isosurfaces) were utilized to delineate the different phases. There are two different types of carbides which were labelled as M_xC_y(I) and M_xC_y(II) respectively, where M stands for metals and M_xC_y denotes the carbides. It is noted that M_xC_y(I) is rich in Mo and M_xC_y(II) is enriched in Cr.

In order to examine the species of carbides from chemistry, three region of interest (ROI) cylinders (i.e. ROI-1, ROI-2 and ROI-3) were created normal to the M_xC_y(I)/M_xC_y(II) and M_xC_y(II)/γ interfaces as illustrated in Fig. 3a. From the 1D concentration profiles in Fig. 3b, c

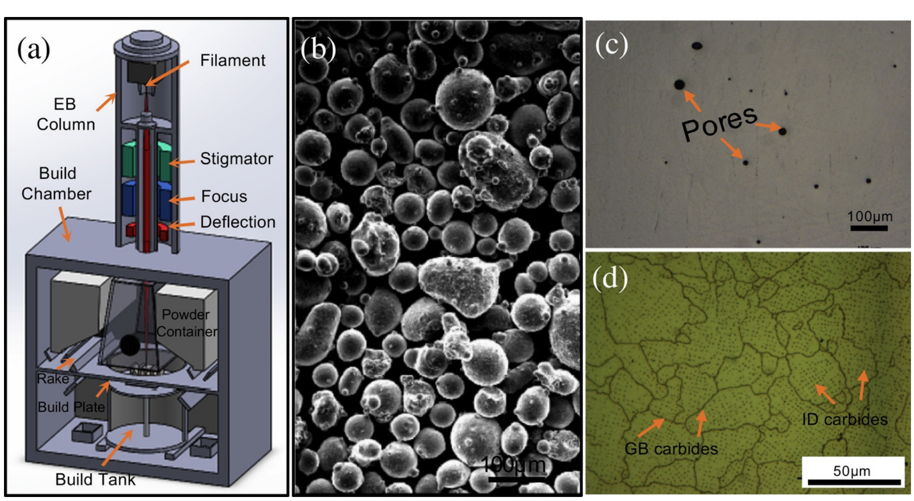

Fig. 1. (a) Schematic of an EBM A2XX system. (b) SEM image of Co-Cr-Mo powder. (c) OM image showing spherical pores in the SEBM-built Co-Cr-Mo sample. (d) OM image showing cross-section microstructure of the SEBM-built Co-Cr-Mo sample. Carbides at grain boundary (GB) and interdendritic (ID) regions were indicated.